RNA–Protein Interactions

DOI: 10.1002/anie.200603284

Inhibition of siRNA Binding to a p19 Viral Suppressor of RNA Silencing by Cysteine Alkylation**

*Selena M. Sagan, Roger Koukiekolo, Elisabeth Rodgers, Natalie K. Goto, and John Paul Pezacki**

The cellular response to double-stranded RNA (dsRNA) is a critical component of the innate immune response to RNA viruses in eukaryotes.[1] An integral component of the dsRNA response is the evolutionarily conserved RNA-silencing response,[1–3] whereby dsRNAs are converted into dsRNAs of approximately 21 nucleotides in length, known as short interfering RNAs (siRNAs), by the enzyme Dicer.[4,5] These siRNAs are then assembled into an RNA-induced silencing complex (RISC),[5,6] which guides the degradation of homologous single-stranded RNA. Viruses that replicate through dsRNA intermediates can trigger the RNA-silencing pathway.[7–9]

Tombusviruses, a family of single-stranded RNA viruses of plants,[10] have developed a mechanism to evade RNA silencing. This mechanism involves a 19-kDa protein (p19), which acts as an siRNA inhibitor.[11,12] The p19 protein binds to and sequesters siRNAs, and by preventing their incorporation into the RISC in this way, effectively turns off the silencing pathway.[11,12] The p19 protein acts as a dimer[11,12] and binds the minor groove of siRNA through interactions with backbone phosphate groups and terminal bases.[11,12] A unique feature of this protein is its ability to bind 21-nucleotide (nt) siRNA with high affinity ($\approx$170 pM) in a size-selective and sequence-independent manner.[12] The ability of p19 to act as a molecular ruler makes it a useful tool for distinguishing between different types of small RNAs; that is, for distinguishing Dicer products, such as siRNAs and microRNAs, from other small RNAs involved in regulatory aspects of the cell, such as rRNAs and tRNAs.

Herein we establish the use of arrays of the p19 protein of carnation Italian ringspot virus (CIRV) for rapid and quantitative detection of CIRV p19–siRNA interactions. These protein arrays allow the size-selective detection of siRNAs and provide a convenient method for screening small-molecule libraries for compounds that can perturb the protein–RNA interaction.

CIRV p19 was first codon optimized for both mammalian and bacterial expression and subcloned into the pTriEx 4-neo vector for bacterial overexpression with a C-terminal histidine tag (p19-H; see the Supporting Information). CIRV p19-H was expressed in *E. coli* BL21 (DE3) cells and was purified on a Ni^{2+}–NTA (NTA = nitrilotriacetate) column. Purified recombinant CIRV p19-H was then captured on 96-well Ni^{2+}–NTA plates at a binding capacity of $\approx$20 pmol per well.

Aliquots of 5′-Cy3-labeled siRNAs were added at increasing concentrations, and the fluorescence of the siRNA that remained bound in each well was measured after a 3-h incubation period. The fraction of bound 5′-Cy3-labeled siRNA was calculated by determining the fraction of the original fluorescence intensity that remained after removal of the unbound 5′-Cy3-labeled siRNA (as outlined in Figure 1). The fluorescence data were fit to Equation (1) to determine

$$f = [\mathrm{siRNA}]_{\max}\left(\frac{[\mathrm{siRNA}]_{\mathrm{U}}}{[\mathrm{siRNA}]_{\mathrm{U}} + K_{\mathrm{d}}}\right) \quad (1)$$

the values of the equilibrium dissociation constant (K_d) for CIRV p19-H–siRNA binding, in which f denotes the relative fluorescence intensity, which is directly proportional to the fractional occupancy of p19, $[\mathrm{siRNA}]_{\max}$ denotes the maximal binding of siRNA, $[\mathrm{siRNA}]_{\mathrm{U}}$ the fraction of unbound siRNA, and K_d the equilibrium dissociation constant. Figure 2a shows

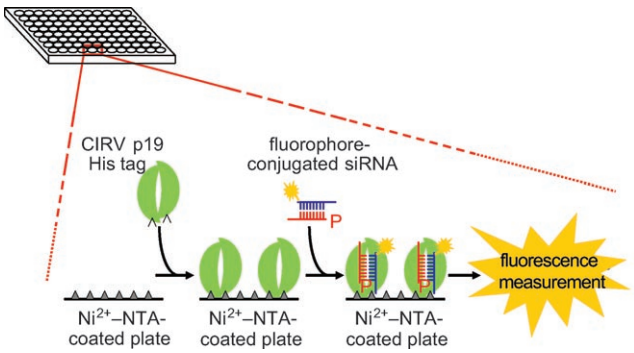

Figure 1. Screening method in the form of a fluorescence-detection assay developed by using the CIRV p19-H protein.

[*] S. M. Sagan,[+] Dr. R. Koukiekolo,[+] E. Rodgers, Prof. J. P. Pezacki
The Steacie Institute for Molecular Sciences
National Research Council of Canada
100 Sussex Drive, Ottawa, K1H 0R6 (Canada)
Fax: (+1) 613-952-0068
E-mail: john.pezacki@nrc-cnrc.gc.ca
Prof. N. K. Goto, Prof. J. P. Pezacki
Department of Chemistry
University of Ottawa
Ottawa, K1N 6N5 (Canada)
S. M. Sagan,[+] Prof. N. K. Goto, Prof. J. P. Pezacki
Department of Biochemistry
Microbiology & Immunology/Ottawa Institute of Systems Biology
University of Ottawa
Ottawa, K1H 8M5 (Canada)
[+] These authors contributed equally to this research.

[**] We thank Y. Rouleau and S. Bélanger for assistance with RNA preparation, P. Bouchard (NRC-BRI) for providing compounds from the Tripos Optiverse Panlab library, and the Genomics and Health Initiative of the NRC for partial funding of this research. S.M.S. thanks the Natural Sciences and Engineering Research Council for funding in the form of a Graduate Scholarship.

Supporting information for this article is available on the WWW under http://www.angewandte.org or from the author.

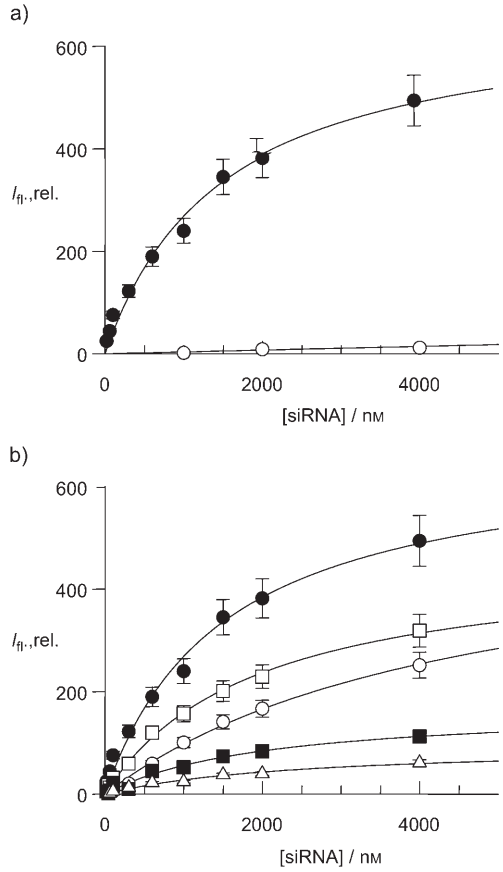

Figure 2. Representative plot and overlayed plots of siRNA binding data for CIRV p19-H fluorescence-detection assays; $I_{fl.,rel.}$ = relative fluorescence intensity. Ninety-six-well microtiter plates containing bound CIRV p19-H were incubated with the following types of siRNA at varying concentrations (0–4 μM): a) a representative Cy3-labeled 21-nt double-stranded siRNA (●) and a corresponding Cy3-labeled 21-nt single-stranded siRNA (○), or b) ds siRNAs of varying lengths: 19-nt GL2 siRNA (○), 21-nt GL2 siRNA (●), 23-nt GL2 siRNA (□), 25-nt GL2 siRNA (■), and 28-nt GL2 siRNA (△). Data points represent the average measurement values from triplicate experiments. Best-fit binding hyperboles are shown with the assumption that one CIRV p19-H dimer binds a single siRNA. All experiments were conducted with the same batch of plates and protein stock solutions to ensure that the saturation point for each well would be the same within experimental error.

a representative graph of the relative fluorescence intensity versus the concentration of the 5′-Cy3-labeled 21-nt siRNA.

To verify that the arrayed CIRV p19-H retained its ability to bind specifically to duplex siRNA, we added 5′-Cy3-labeled single-stranded siRNAs in increasing concentrations to wells with immobilized CIRV p19-H (Figure 2a). Reaction wells containing 5′-Cy3-labeled 21-nt single-stranded siRNA designed to target the firefly luciferase gene (GL2) gave very low levels of fluorescence (Figure 2a, ○), whereas fluorescence of a significant intensity was observed with 5′-Cy3-labeled 21-nt GL2-targeting duplex siRNA over the range of concentrations tested (Figure 2a, ●). This result illustrates that the arrayed CIRV p19-H binds specifically to double-stranded siRNAs rather than to the corresponding single-stranded siRNAs, as demonstrated previously.[12] To determine whether our immobilized p19 also binds to ds siRNAs in a sequence-independent manner, we evaluated interactions of CIRV p19-H with a range of 21-nt siRNAs of unrelated sequences (see the Supporting Information). We determined apparent K_d values of CIRV p19-H for 21-nt ds siRNA molecules that target GL2, CSK-2 (human Src kinase), and 331 (the 5′ untranslated region of the hepatitis C) by fitting the data for fluorescence versus siRNA concentration (see the Supporting Information) to Equation (1). We found that immobilized CIRV p19-H bound to all ds 21-nt siRNAs with a similar affinity, with apparent K_d values of 600–1200 nM. This result confirms that arrayed CIRV p19-H binds to 21-nt ds siRNA in a sequence-independent manner.

We also tested the size selectivity of CIRV p19-H binding by using ds siRNAs of various lengths (19-, 21-, 23-, 25-, and 28-nt GL2-targeting siRNAs). Plate-bound CIRV p19-H showed the highest affinity for 21-nt ds siRNA with progressively declining affinities for siRNAs of greater or shorter lengths (Figure 2b). This trend is in agreement with that observed previously in electrophoretic mobility shift assays (EMSA) with radiolabeled siRNAs of varying lengths.[12,13]

Next, we screened 500 compounds from the Tripos Optiverse Panlabs library for inhibitors of the binding of CSK-2 ds siRNA to CIRV p19-H, as this siRNA exhibited the highest affinity in our assay. Two compounds were found to inhibit CSK-2 siRNA interactions with CIRV p19-H to a larger degree than the positive control (unlabeled CSK-2 ds siRNA). Further investigation of both compounds showed that they inhibited the binding of siRNA in a concentration-dependent manner with IC_{50} values in the μM range (see the Supporting Information).

A mechanism for CIRV p19 inhibition can be proposed on the basis of the presence of thiosulfonate functional groups in both identified inhibitors (Figure 3). Since thiosulfonate

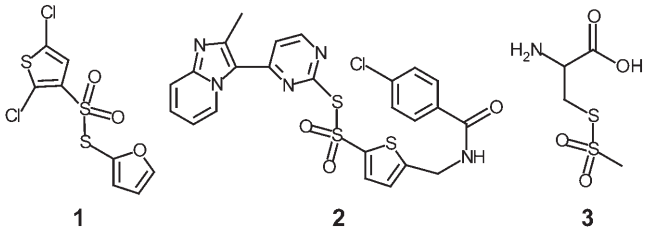

Figure 3. Structures of the two thiosulfonates identified from the Tripos Optiverse Panlab library that block CIRV p19–siRNA interactions (compounds **1** and **2**), and a model thiosulfonate **3** used for MALDI MS analyses.

groups are reactive toward cysteine residues,[14] the inhibition of p19–siRNA interactions could be attributed to the covalent modification of p19 according to Equation (2).

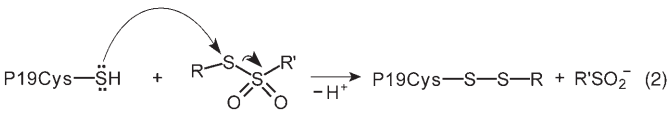

To determine whether covalent modification of cysteine residues could inhibit CIRV p19 activity, we investigated the effect of cysteine alkylation by *N*-ethylmaleimide on CIRV p19-H–siRNA binding. According to MALDI MS analysis of samples treated with *N*-ethylmaleimide, most of the CIRV p19 was alkylated at two sites per monomer. When the ability of this alkylated sample to bind siRNA was evaluated in our fluorescence assay, we found that there was a greater than tenfold reduction in siRNA binding (see the Supporting Information), which suggests the modification of CIRV p19 Cys residues as a mechanism for the inhibition of siRNA binding. By using model compound **3** as well as compound **1**, we also established that molecules containing thiosulfonate functional groups can alkylate p19. Depending on the incubation time and number of equivalents, we observed by MALDI MS mass increases that correspond to between one and four alkylations per p19 dimer (see the Supporting Information). Thus, we deduced that compound **1** is a covalent inhibitor.

Inspection of the CIRV p19 X-ray crystal structure[12] provides some insight into how the covalent modification of a cysteine residue could inhibit siRNA binding. One of the possible sites of modification is Cys110, which is located in the siRNA-binding pocket (Figure 4). We postulate that

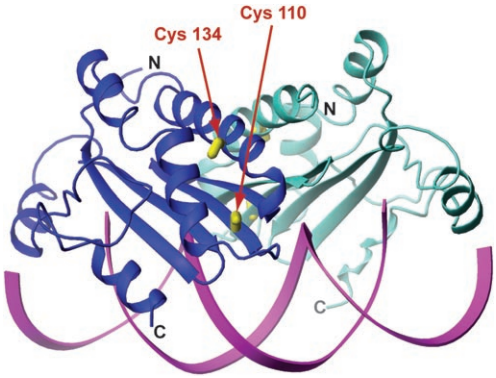

Figure 4. A ribbon diagram of the CIRV p19 crystal structure (PDB code: 1RPU) with the side chains of Cys110 and Cys134 highlighted in yellow. Cys160 is located in the flexible C-terminal region, which was not resolved in the crystal structure.

modification at this site would change the chemical and structural properties of this functionally important region. Although modification at Cys134 could also be responsible for inhibition, its location far from the siRNA-binding site makes it less likely to interfere with p19 activity; however, indirect inhibition through destabilization of the p19 structure is a possibility that can not be ruled out. Interestingly, the side chains of both Cys134 and Cys110 are oriented towards the protein interior in an environment that would be predicted to be inaccessible to alkylating agents on the basis of the crystal structure. Although a crystal structure of p19 without siRNA is not available, our results indicate that one of these regions becomes solvent accessible, potentially as a result of a conformational change, when siRNA is not bound.

In summary, we have demonstrated that the siRNA-suppressor protein CIRV p19 can be arrayed in multiwelled plates through interactions of Ni^{2+}–NTA with the His tag and these arrayed proteins can be used to rapidly determine relative siRNA-binding affinities. The arrayed CIRV p19-H maintains its ability to act as a molecular ruler by binding siRNAs in a size-selective, sequence-independent manner. Furthermore, the screening of a library of small molecules identified two inhibitors of CIRV p19 activity that may act through the modification of a cysteine residue. One of the most plausible sites of modification is Cys110, which is located in the siRNA-binding pocket and is the only cysteine residue that is conserved among the entire p19 family. As other hydrophobic residues should be capable of fulfilling the structural role of this residue, Cys110 may be required for a different type of biological function. One possibility raised by the results of our library screen is that redox switching by physiological thiols, such as glutathione, could allow reversible inactivation of p19. Such regulation could influence the site of action of p19 and minimize nonproductive binding of RNAs. Therefore the multiwell assay described herein not only identified compounds that could serve as a starting point for the development of covalent inhibitors of CIRV p19 with enhanced target selectivity, but has also given rise to new postulates regarding the regulation of p19 in vivo.

Experimental Section

Protein expression and purification: The p19 protein of carnation Italian ringspot virus (CIRV) was codon optimized for both mammalian and bacterial expression and synthesized by Genescript Corporation (Piscataway, NJ) in plasmid vector pUC57 (for the CIRV p19 sequence, see the Supporting Information). CIRV p19 was subsequently subcloned by PCR into the pTriEx 4-neo vector (EMD Biosciences, San Diego, CA) by using forward (5′-TAAGCCATG-GAACGCGCTATCCAAGG-3′) and reverse (5′-CGACTC-GAGCTCGCTTTCTTTCTTGAAGG-3′) PCR primers. The CIRV p19 PCR product was digested with *NcoI* and *XhoI* and inserted into the multiple cloning site of pTriEx 4-neo with a C-terminal 8X histidine tag. The resulting CIRV p19 pTriEx 4-neo (pTriEx-p19) plasmid construct was confirmed by sequencing.

Bacterial overexpression of CIRV p19 with a histidine tag (p19-H) was carried out at 37 °C in cells of the *E. coli* strain BL21 (DE3) that harbored the pTriEx-p19. Expression of CIRV p19-H was induced by isopropyl-β-D-thiogalactopyranoside (IPTG) at a final concentration of 1 mM. Cultures were then grown for an additional 4–5 h at 30 °C. Bacterial pellets were resuspended in lysis buffer (NaH_2PO_4 (50 mM), NaCl (300 mM), imidazole (10 mM), lysozyme (1 mg mL^{-1}), pH 8.0) and lysed by sonication on ice. The CIRV p19-H protein was purified from the soluble fraction of lysate by binding to a Ni^{2+}–NTA column (Pharmacia, Peapack, NJ). The resin was washed with wash buffer I (NaH_2PO_4 (50 mM), NaCl (500 mM), imidazole (20 mM), pH 8.0), then with wash buffer II (NaH_2PO_4 (50 mM), NaCl (300 mM), 20% glycerol, pH 8.0), and finally with wash buffer III (NaH_2PO_4 (50 mM), NaCl (300 mM), 1% Tween-20, pH 8.0). CIRV p19-H was eluted with elution buffer (NaH_2PO_4 (50 mM), NaCl (300 mM), imidazole (250 mM), pH 8.0). The pooled eluates were desalted by using a PD-10 column (Pharmacia, Peapack, NJ) and concentrated into 1 mL of Tris–HCl buffer (50 mM, pH 8.0; Tris = tris(hydroxymethyl)aminomethane) by using an Ultrafree 10-kDa membrane (Millipore, Concord, MA).

For Western blot analysis, CIRV p19-H overexpression was induced by IPTG (1 mM) in *E. coli* BL21 (DE3) cells, and aliquots

were taken at 1, 0.5, 1, 2, and 4 h postinduction. Cells transformed with the pTriEx 4-neo vector were used as a negative control. Aliquots were diluted in SDS-PAGE loading buffer (Tris–HCl (50 mM, pH 6.8), 2% SDS, 10% glycerol, dithiothreitol (DTT; 1 mM), 0.1% bromophenol blue), and 25 μL of sample per well was loaded for SDS-PAGE (12% resolving, 4% stacking gel). The resolved proteins were transferred to a Hybond-P polyvinylidene difluoride membrane (Amersham Biosciences, Piscataway, NJ). The membrane was blocked with 5% skim milk in TBS–Tween (TBS = Tris-buffered saline) and probed for the CIRV p19-H C-terminal histidine tag with a monoclonal anti-polyhistidine primary antibody (1.5 $\mu g\,mL^{-1}$, R&D Systems, Inc., Minneapolis, MN) followed by a secondary HRP-conjugated goat antimouse IgG antibody (1:1000 dilution; HRP = horseradish peroxidase) obtained from Jackson ImmunoResearch Laboratories Inc. (Westgrove, PA). Protein bands were visualized by using Western Lightning Western blot chemiluminescence reagents (PerkinElmer Life and Analytical Sciences, Inc, Boston, MA) according to the protocol of the manufacturer.

Fluorescence-detection assays and data analysis: Fluorescence-detection assays were carried out by using 96-well Ni^{2+}–NTA plates (Qiagen Inc., Mississauga, Ontario). With respect to the binding specificity, a small peptide ($\approx$12 kDa) from the native pTriEx 4-neo vector sequence that corresponded to the multiple cloning site (MCS) of pTriEx 4-neo and included an 8X His tag at the 3′ end was overexpressed and purified as described for CIRV p19-H. Purified CIRV p19-H or small peptide (200 μl, 10 $\mu g\,mL^{-1}$) in 1X PBS (phosphate-buffered saline), 0.2% bovine serum albumin (BSA), pH 7.2, was prebound to the surface of each well of the Ni^{2+}–NTA-coated 96-well plate by treatment for 3 h at room temperature. Wells were then washed twice with wash buffer (1X PBS containing Tween 20 (0.05%) and EDTA (ethylenediaminetetraacetic acid; 1 mM)). The composition of the wash buffer and washing conditions were optimized to minimize nonspecific binding, maximize signal fluorescence, and lower background fluorescence. 1X PBS (0.2% BSA, pH 7.2; 200 μL) was then placed in each well, and the background fluorescence ($E_x = 546$ nm, $E_m = 590$ nm) was measured with a Spectramax M2 plate reader (Molecular Devices Corporation, Sunnyvale, CA) for normalization purposes. The wells were then washed once more with wash buffer before the addition of the siRNAs. The Cy3-labeled siRNAs (0–4 μM, diluted in 1X PBS (0.2% BSA, pH 7.2)) were then added to each well, and the plates were incubated in the dark for 3 h at room temperature. Wells were then washed four times with wash buffer, and 1X PBS, 0.2% BSA, pH 7.2, 200 μL was placed into each well for fluorescence measurement. Fluorescence detection of bound Cy3-labeled siRNAs ($E_x = 546$ nm, $E_m = 590$ nm) was measured with a Spectramax M2 plate reader. The relative fluorescence of specific binding was calculated by subtracting the nonspecific value for the fluorescence of siRNA binding to the small peptide from the measured fluorescence of siRNA binding to CIRV p19-H. Although we have optimized the washing steps, it is possible that siRNA off rates may contribute to discrepancies between apparent dissociation constants.

We verified the specific binding of the His tag of CIRV p19-H to the Ni^{2+}–NTA-coated wells by adding imidazole at varying concentrations (0–100 mM) to the Ni^{2+}–NTA-coated wells prior to the addition of CIRV p19-H and fluorescently tagged siRNAs. In the presence of 100 mM imidazole we were only able to detect less than 10% total binding of Cy3-labeled siRNA at saturating siRNA concentrations. To ensure that the fluorescence measured for siRNA binding was due to a specific interaction with CIRV p19-H, a random approximately 12 kDa polypeptide sequence containing a His_8 tag was subjected to the same expression, purification, and assay procedures as utilized for CIRV p19-H. Negligible fluorescence was observed. Additionally, by using the array-based approach, CIRV-p19 was immobilized in Ni^{2+}–NTA-coated wells. When relative K_d values of binding between different siRNA molecules were compared, experiments were conducted with the same batches of plates and the same stock solution of protein to ensure that the saturation point for each well was the same within experimental error. In some cases saturation binding (i.e. the determination of $[siRNA]_{max}$) was impossible to achieve as a result of the prohibitively high cost of producing sufficient quantities of siRNA. In these cases the potential error in the K_d values from this uncertainty in $[siRNA]_{max}$ was evaluated by measuring the saturation binding for a generic siRNA on the same surfaces with the same protein samples. For all reported K_d values, the results obtained from curve fitting performed with and without the $[siRNA]_{max}$ measured with generic siRNA were found to be the same within experimental error.

Screening of the small-molecule compound library: The binding of purified CIRV p19-H to Ni^{2+}–NTA plates was carried out as described for fluorescence-detection assays. After the washing and normalization steps, compounds from the Tripos Optiverse Panlabs library (NRC-BRI, Montreal, Quebec) were added at 100 μM in 1X PBS to each well. (A different compound was added to each well of the plate). The plates were then incubated for 2 h at room temperature in the dark. Wells were then washed four times with wash buffer, and 1X PBS, 0.2% BSA, pH 7.2, 200 μL was placed into each well for normalization measurements ($E_x = 546$ nm, $E_m = 590$ nm) with a Spectramax M2 plate reader. Cy3-labeled siRNAs (21-nt CSK-2 siRNA (1 μM), diluted in 1X PBS, 0.2% BSA, pH 7.2) were then added to each well, and the plates were incubated in the dark for 2 h at room temperature. Wells were then washed four times with wash buffer, and 1X PBS, 0.2% BSA, pH 7.2, 200 μL was placed into each well for fluorescence measurement. Fluorescence detection of bound Cy3-labeled siRNAs ($E_x = 546$ nm, $E_m = 590$ nm) was measured with a Spectramax M2 plate reader. The increased emission wavelength of $E_m = 590$ nm rather than the reported $E_m = 565$ nm for Cy3 was used to minimize background fluorescence. Postincubation experiments in which the treatment with compounds was carried out after siRNA binding were also conducted. All experiments in which compounds were added were carried out in triplicate. As controls, fluorescence was measured from wells containing CIRV p19-H alone as well as unlabeled CSK-2 siRNAs.

Treatment with *N*-ethylmaleimide: Treatment with *N*-ethylmaleimide was carried out in 96-well Ni^{2+}–NTA plates as for fluorescence detection assays. The binding of purified CIRV p19-H to Ni^{2+}–NTA plates was carried out as described for fluorescence-detection assays. After the washing and normalization steps, *N*-ethylmaleimide in 1X PBS (20 mM, 200 μL) was incubated with the prebound CIRV p19-H for 2 h with gentle shaking at room temperature. Wells were then washed twice with wash buffer. 1X PBS, 0.2% BSA, pH 7.2, 200 μL was then placed in each well, and the background fluorescence ($E_x = 546$ nm, $E_m = 590$ nm) was measured with a Spectramax M2 plate reader for normalization purposes. The wells were then washed once more with wash buffer before the addition of the siRNAs. The Cy3-labeled siRNAs (0–4 μM, diluted in 1X PBS, 0.2% BSA, pH 7.2) were then added to each well, and the plates were incubated in the dark for 3 h at room temperature. Wells were then washed four times with wash buffer, and 1X PBS, 0.2% BSA, pH 7.2, 200 μL, was placed into each well for fluorescence measurement. Fluorescence detection of bound Cy3-labeled siRNAs ($E_x = 546$ nm, $E_m = 590$ nm) was measured with a Spectramax M2 plate reader.

Graphs and data analysis: All graph analyses were performed by using the Graph-Pad Prism computer program (San Diego, CA, USA).

MALDI-TOF MS analysis: For MALDI-TOF protein analysis, either purified CIRV p19-H (0.5 μg) or CIRV p19-H (0.5 μg) incubated with (*R*)-2-amino-2-carboxyethylmethanethiosulfate (**3**) for 1–24 h at room temperature in a 1:1 or 1:10 ratio was analyzed. Similar experiments were conducted with purified CIRV p19-H (0.5 μg) incubated with the inhibitor **1** in a 1:1 ratio. All experiments were performed in acetate ammonium buffer (10 mM, pH 7.5) with preincubation for 2 h at 4 °C in a final volume of 10 μL. For MALDI-TOF analysis of maleimide-modified p19, purified CIRV p19-H

(0.5 μg) was incubated with *N*-ethylmaleimide (50 mM) for 2 h at 4 °C, and the mixture was diluted to a final volume of 10 μL for analyses. All experiments were performed in acetate ammonium buffer (10 mM, pH 7.5). One microliter of each sample was mixed with sinapinic acid matrix (60 mg mL^{-1} in 30% EtOH; 10 μL), and the resulting mixture was spotted on a steel target plate and air dried at room temperature. Mass spectrometry was performed on a Voyager-DE STR MALDI-TOF instrument (Applied Biosystems, Foster City, CA) operated in the linear/positive mode.

Received: August 10, 2006
Revised: December 4, 2006
Published online: February 8, 2007

Keywords: chemical probes · fluorescence · RNA silencing · RNA–protein interactions · viruses

[1] G. J. Hannon, *Nature* **2002**, *418*, 244 – 251.
[2] A. Fire, S. Q. Xu, M. K. Montgomery, S. A. Kostas, S. E. Driver, C. C. Mello, *Nature* **1998**, *391*, 806 – 811.
[3] P. D. Zamore, T. Tuschl, P. A. Sharp, D. P. Bartel, *Cell* **2000**, *101*, 25 – 33.
[4] E. Bernstein, A. A. Caudy, S. M. Hammond, G. J. Hannon, *Nature* **2001**, *409*, 363 – 366.
[5] S. M. Elbashir, J. Harborth, W. Lendeckel, A. Yalcin, K. Weber, T. Tuschl, *Nature* **2001**, *411*, 494 – 498.
[6] S. M. Hammond, E. Bernstein, D. Beach, G. J. Hannon, *Nature* **2000**, *404*, 293 – 296.
[7] S. N. Covey, N. S. Al-Kaff, A. Langara, D. S. Turner, *Nature* **1997**, *385*, 781 – 782.
[8] F. Ratcliff, B. D. Harrison, D. C. Baulcombe, *Science* **1997**, *276*, 1558 – 1560.
[9] F. G. Ratcliff, S. A. MacFarlane, D. C. Baulcombe, *Plant Cell* **1999**, *11*, 1207 – 1215.
[10] M. Russo, J. Burgyan, G. P. Martelli, *Adv. Virus Res.* **1994**, *44*, 381 – 428.
[11] Q. Ge, M. T. McManus, T. Nguyen, C. H. Shen, P. A. Sharp, H. N. Eisen, J. Z. Chen, *Proc. Natl. Acad. Sci. USA* **2003**, *100*, 2718 – 2723.
[12] J. M. Vargason, G. Szittya, J. Burgyan, T. M. T. Hall, *Cell* **2003**, *115*, 799 – 811.
[13] D. Silhavy, A. Molnar, A. Lucioli, G. Szittya, C. Hornyik, M. Tavazza, J. Burgyan, *Embo J.* **2002**, *21*, 3070 – 3080.
[14] K. Peters, F. M. Richards, *Annu. Rev. Biochem.* **1997**, *66*, 523 – 551.

